

Supplementary Materials for

Toughening stretchable fibers via serial fracturing of a metallic core

Christopher B. Cooper, Ishan D. Joshipura, Dishit P. Parekh, Justin Norkett, Russell Mailen, Victoria M. Miller, Jan Genzer, Michael D. Dickey*

*Corresponding author. Email: mddickey@ncsu.edu

Published 22 February 2019, *Sci. Adv.* **5**, eaat4600 (2019)
DOI: 10.1126/sciadv.aat4600

The PDF file includes:

Note S1. Quantitative characterization of the metamaterial fiber stress-strain behavior.
Note S2. Full derivation of model.
Fig. S1. Detailed schematic of metamaterial fiber behavior.
Fig. S2. Stress-strain curves for Ga-only, SEBS-only, and Ga-SEBS fibers.
Fig. S3. Linear regression of aggregated stress-strain data from metamaterial fibers.
Fig. S4. Scalability of metamaterial fibers.
Fig. S5. Simultaneous straining of two metamaterial fibers.
Fig. S6. Metamaterial fiber composed of a gallium core and a silicone polymer shell.
Fig. S7. Second-order polynomial regression for a hollow SEBS fiber.
Fig. S8. Optical images of a relaxed metamaterial after straining.
Table S1. Comparison of mechanical properties with SDs, 95% confidence intervals, and sample sizes.
Legends for movies S1 to S3

Other Supplementary Material for this manuscript includes the following:

(available at advances.sciencemag.org/cgi/content/full/5/2/eaat4600/DC1)

Movie S1 (.mp4 format). Elongation of a metamaterial fiber.
Movie S2 (.mp4 format). Slipping mechanism for the formation of polymer bridges.
Movie S3 (.mp4 format). Demonstration of a metamaterial fiber.

Note S1. Quantitative characterization of the metamaterial fiber stress-strain behavior.

The repetitive sawtooth shape of the stress-strain curve suggests that the behavior of the metamaterial fibers can be characterized approximately as waves with a certain period and amplitude. Indeed, after the first fracture in the metal core, the subsequent fractures occur at a fairly steady interval and amplitude. By calculating the amount of macroscopic extension between breaks in the metal core for many fibers, we determined that the average increase in macroscopic strain between any two breaks (*i.e.*, the period) was 32%. Similarly, the average decrease in stress that occurs after each fracture (*i.e.*, the amplitude) is 0.8 MPa. Knowing that the fibers maintain an average stress of 3.9 MPa, we can combine this information to describe the general behavior of the fibers. After the first break, the fiber exhibits a sawtooth-shaped oscillation centered at a stress of 3.9 MPa with an amplitude of 0.8 MPa (*i.e.*, drops from 4.3 MPa to 3.5 MPa and then returns to 4.3 MPa) and a period of 32% macroscopic strain (*i.e.*, a break occurs with every 32% increase in macroscopic strain).

Note S2. Full derivation of model.

We considered two things that must be true: (1) At any cross-section of the fiber, the net force must be equal to the force (F) exerted by the grips of the extensometer at the ends of the fiber. (2) The sum of the lengths in the individual regions must sum to the total length (L) of the fiber.

We define the macroscopic or global strain (represented by the change in distance between the extensometer grips) as

$$\varepsilon = \frac{L-L_0}{L_0} \quad (\text{S1})$$

where L_0 is the initial length of the fiber (*i.e.*, length at zero strain). A fiber with an outer radius (r_f) and an inner radius (r_m) has an initial cross sectional area of the fiber (A_f), of the metal core (A_m), and of the polymer shell (A_p) as

$$A_p = A_f - A_m = \pi r_f^2 - \pi r_m^2 \quad (\text{S2})$$

Then the engineering stress in the fiber is given by

$$\sigma_f = \frac{F}{A_f} \quad (\text{S3})$$

After the first break in the metal core occurs, there are two types of regions in the fiber: (1) metal segments surrounded by an encasing polymer shell, and (2) polymer bridges. Since these polymer bridges must support the entire force (F) exerted by the extensometer, the engineering stress in the polymer bridges is

$$\sigma_p = \frac{F}{A_p} \quad (\text{S4})$$

We can approximate the relationship between stress (σ_p) and strain (ε_p) in the polymer by

$$\sigma_p = c_2 \varepsilon_p^2 + c_1 \varepsilon_p + c_0 \quad (\text{S5})$$

Where c_0 , c_1 , and c_2 are constants found by the fitting a second-order polynomial to a stress-strain curve for a hollow SEBS fiber (see fig. S7 for more details). We can rewrite Eq. (S5) using the quadratic formula to determine the amount of strain in the polymer bridges for a given stress (after plugging in values for the constants, the negative root can be ignored)

$$\varepsilon_p = \frac{-c_1 + \sqrt{c_1^2 - 4c_2(c_0 - \sigma_p)}}{2c_2} \quad (\text{S6})$$

Since force is constant at all cross sections of the fiber, the engineering stress (and by Eq. (S6) the strain as well) in all polymer bridges is the same. This does not guarantee that each polymer bridge is the same length (in fact, they are not), since the encasing polymer shell can slip by different amounts for different polymer bridges. However, if we know the length of a single polymer bridge ($l_{p,i}$), we can calculate its length at (hypothetical) zero strain ($l_{p0,i}$) as

$$l_{p0,i} = \frac{l_{p,i}}{1 + \varepsilon_p} \quad (\text{S7})$$

This value represents the ‘initial’ length of the polymer bridge (*i.e.*, its length in the absence of stress) and is a quantitative measure of the magnitude by which the encasing polymer has been transferred between the metal core segments to form polymer bridges.

The total length of k metal segments is given by

$$L_m = \sum_{j=1}^k l_{m,j} \quad (\text{S8})$$

The total length of n polymer bridges is given by

$$L_p = \sum_{i=1}^n l_{p,i} = L - L_m \quad (\text{S9})$$

which can be used to calculate the total initial length of the polymer bridges (*i.e.*, the total amount of encasing polymer that has been transferred into all of the polymer bridges) with

$$L_{po} = \frac{L_p}{1+\varepsilon_p} \quad (\text{S10})$$

Since each metal segment is encased in a polymer shell, the total length of the encasing polymer is simply equal to

$$L_p^e = L_m \quad (\text{S11})$$

Similar to our analysis of the polymer bridges, we can calculate the initial length of the encasing polymer (*i.e.*, the length at hypothetical zero strain) by noting that the total initial length of polymer is equal to the initial length of the fiber and that all of the polymer not transferred to polymer bridges must still be in the encasing polymer shell. This yields

$$L_{po}^e = L_o - L_{po} \quad (\text{S12})$$

We can then calculate the strain in the encasing polymer (which differs from the strain in the polymer bridges) as

$$\varepsilon_p^e = \frac{L_p^e - L_{p0}^e}{L_{p0}^e} \quad (\text{S13})$$

Using Eq. (S5), we can determine the amount of engineering stress in the encasing polymer (σ_p^e), which can then be used in Eq. (S4) to determine the force on the encasing polymer (F_p^e). Noting that the difference between the force on the fiber and the force on the encasing polymer must be the force on the metal core, we arrive at

$$F_m = F - F_p^e \quad (\text{S14})$$

Which can be used to calculate the engineering stress in the metal

$$\sigma_m = \frac{F_m}{A_m} \quad (\text{S15})$$

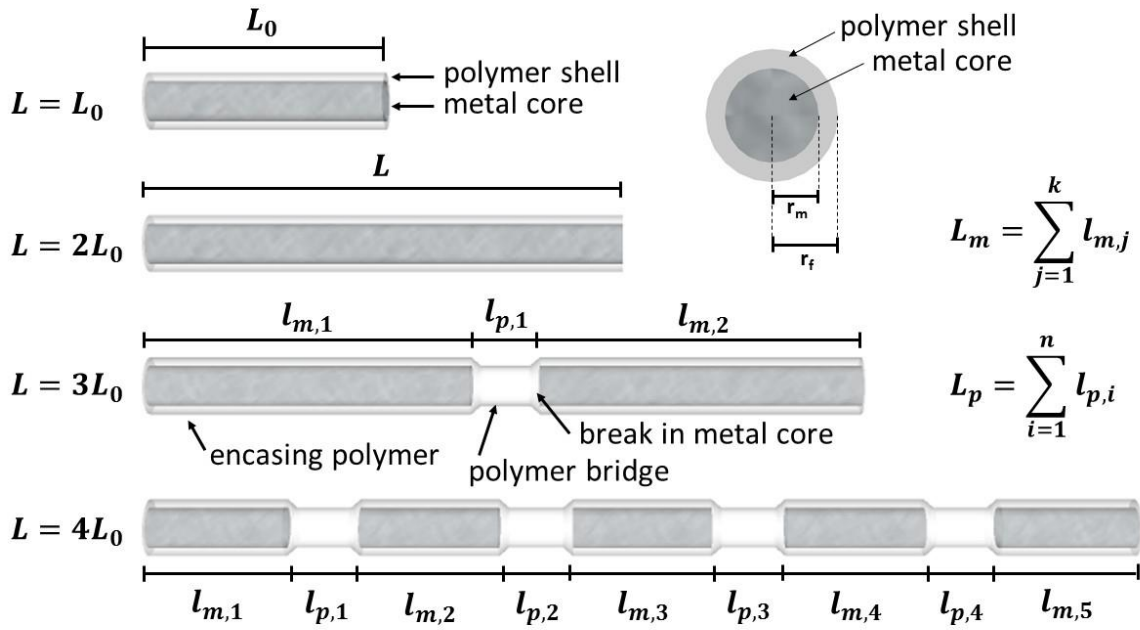


Fig. S1. Detailed schematic of metamaterial fiber behavior. This schematic contains additional labels (compared to Fig. 1A) that identify the individual polymer bridges and metal segments as well as formulas for L_m and L_p .

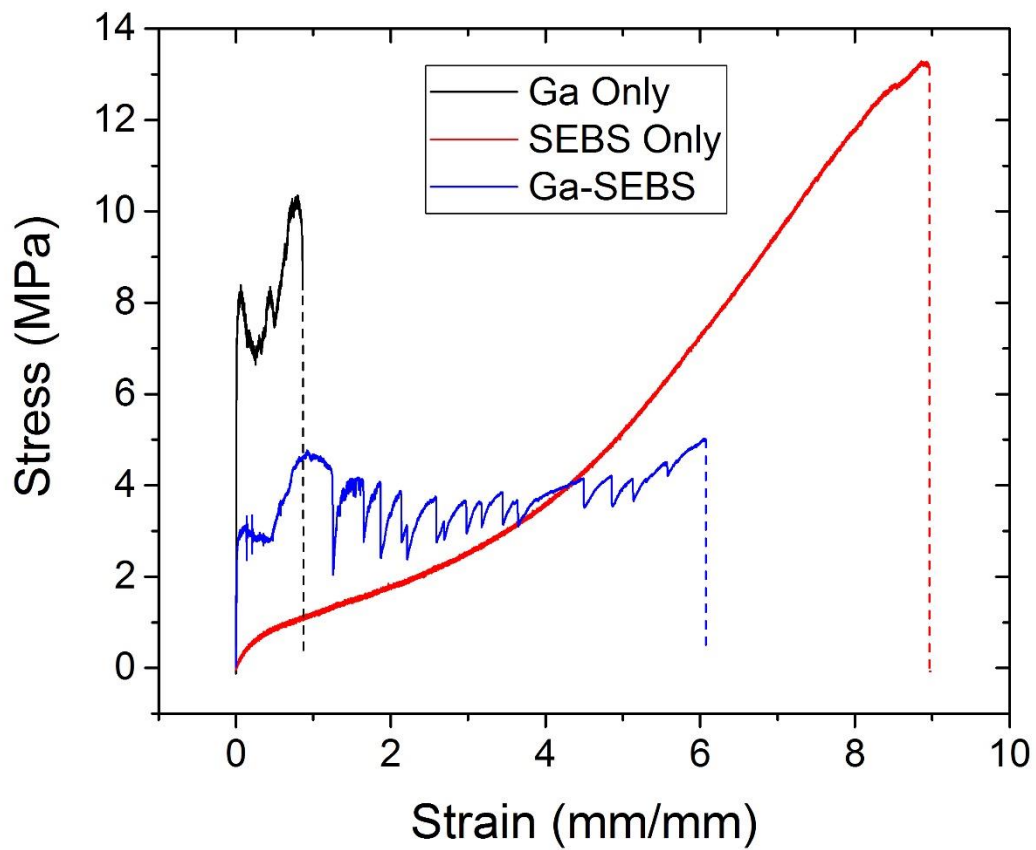


Fig. S2. Stress-strain curves for Ga-only, SEBS-only, and Ga-SEBS fibers. Stress is the measured force normalized by the cross-sectional area (thus, the stress of the Ga-SEBS fiber appears artificially lower than the Ga fiber even though they require similar force to extend).

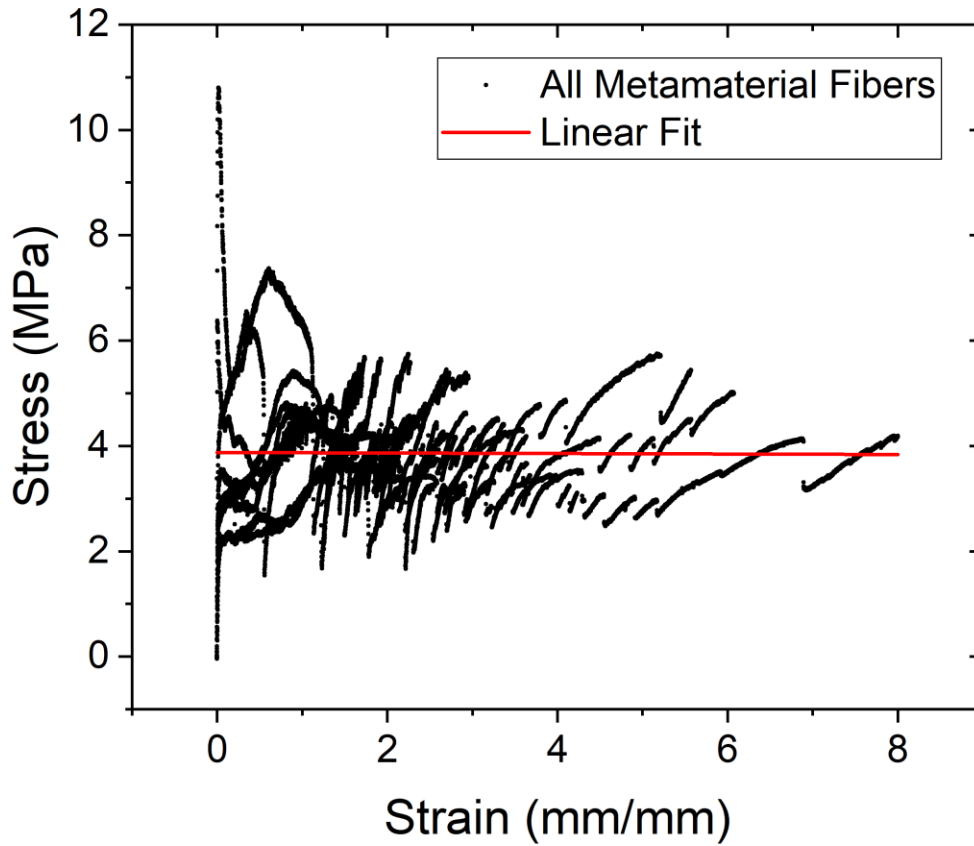


Fig. S3. Linear regression of aggregated stress-strain data from metamaterial fibers. The resulting horizontal line has a value of 3.9 MPa, the average stress held by a metamaterial fiber. As the variation between individual fibers is significant, the fitting has an R^2 value of 0.

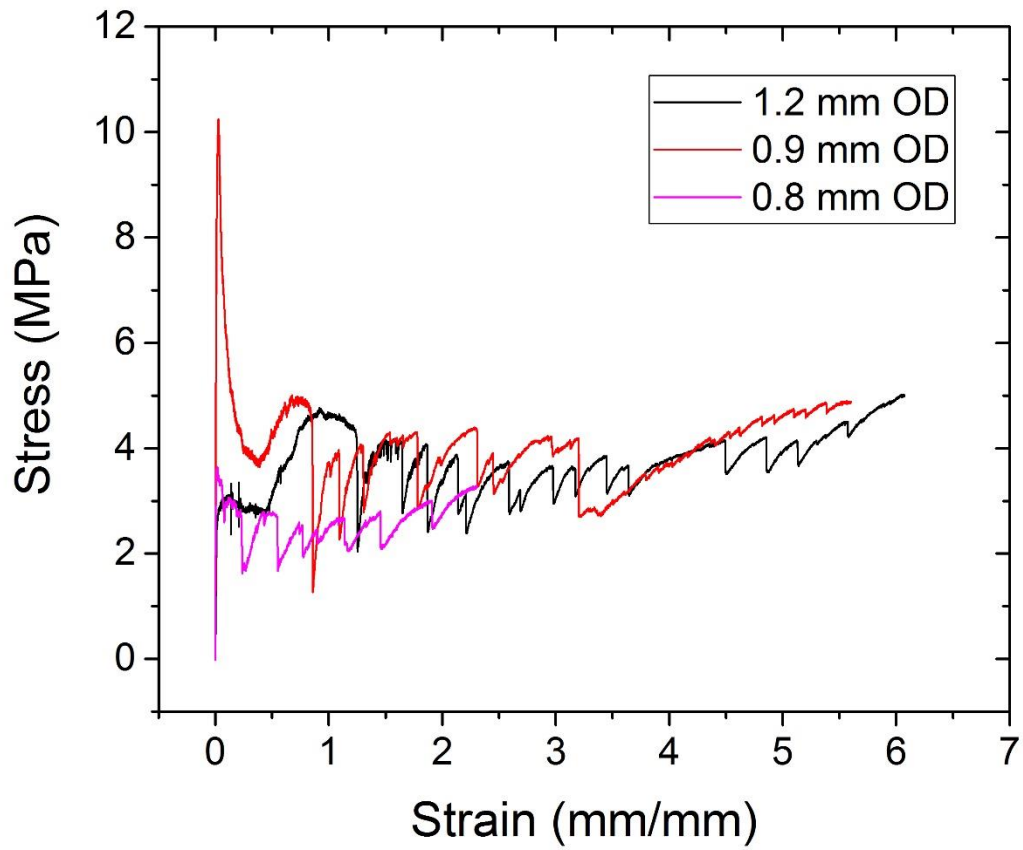


Fig. S4. Scalability of metamaterial fibers. The graph plots the stress-strain curves for three fibers with outer diameters (OD) of 0.8, 0.9, and 1.2 mm, showing that the behavior of the metamaterial fiber is consistent and scalable.

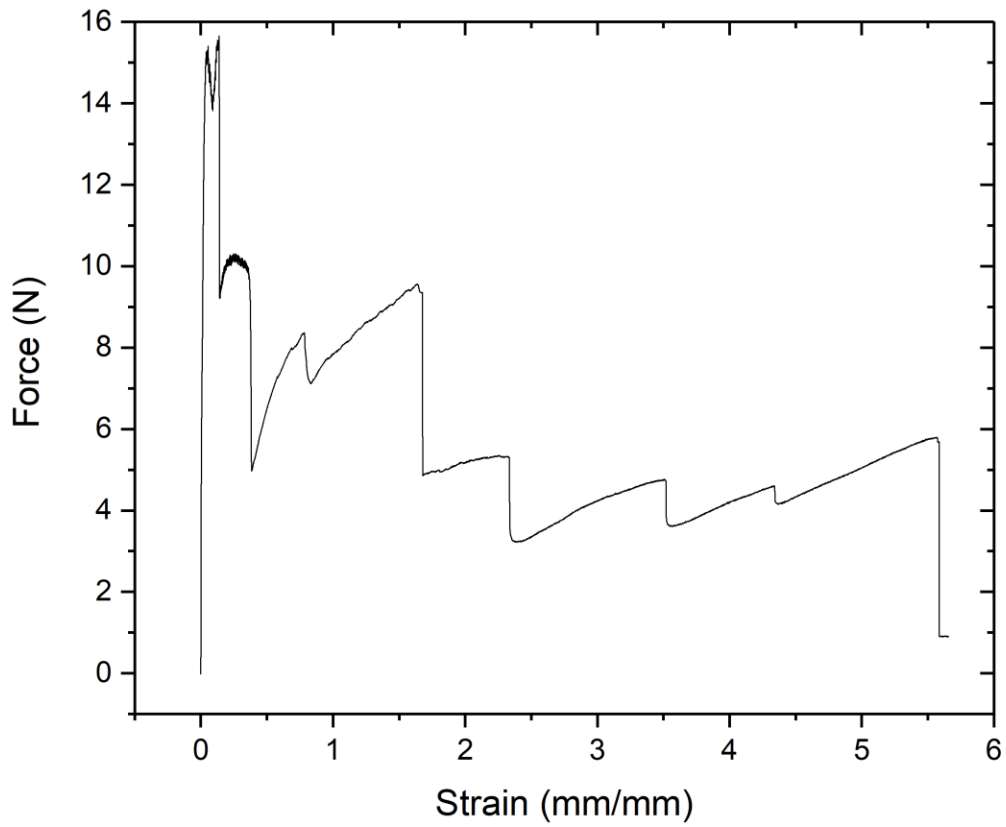


Fig. S5. Simultaneous straining of two metamaterial fibers. The graph plots the force-strain curve for a pair of metamaterial fibers strained simultaneously, showing that the set of fibers exhibits metamaterial behavior up to 550% strain.

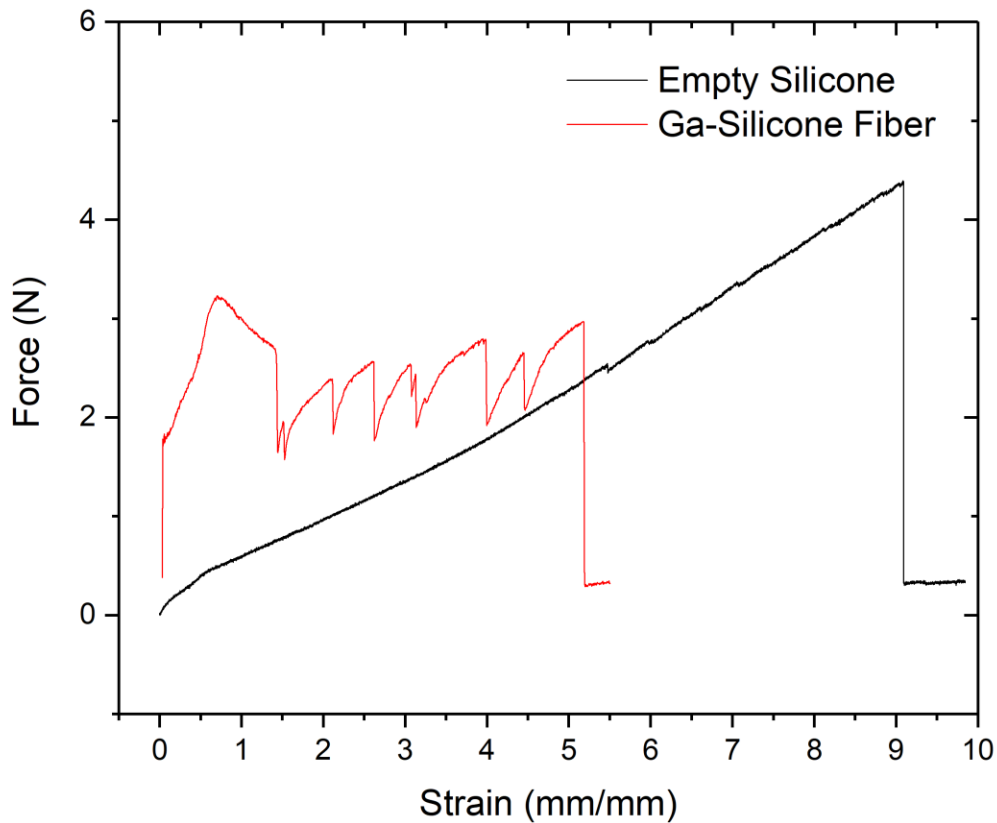


Fig. S6. Metamaterial fiber composed of a gallium core and a silicone polymer shell. The graph plots the force-strain curve for hollow (black) and gallium-filled (red) silicone fibers with an OD of 0.94 mm and an ID of 0.51 mm. The gallium-filled silicone fiber exhibits metamaterial behavior, holding an average force of 2.4 N up to 500% strain and exhibiting enhanced toughness compared to the hollow silicone fiber. Given the reduced cross-sectional area of the gallium core in the silicone fiber, this agrees nicely with the reported Ga-SEBS metamaterial fiber results and demonstrates that the metamaterial behavior is not limited to only SEBS polymer shells.

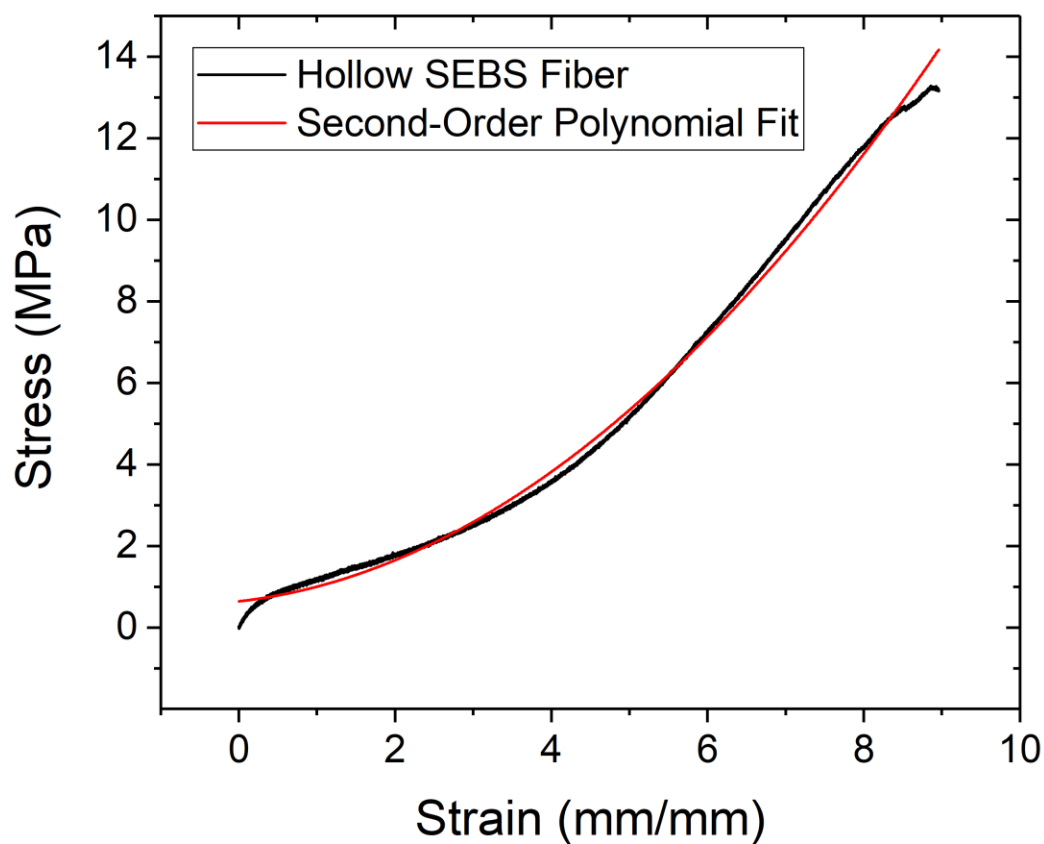


Fig. S7. Second-order polynomial regression for a hollow SEBS fiber. The regression gives the values for c_0 , c_1 , c_2 in Eq. (S5), where $c_0 = 0.64825$ MPa, $c_1 = 0.21513$ MPa, and $c_2 = 0.14447$ MPa. The fitting has an R^2 value of 0.99. This fit is useful for relating strain to stress in the polymer component of the fiber during extension.

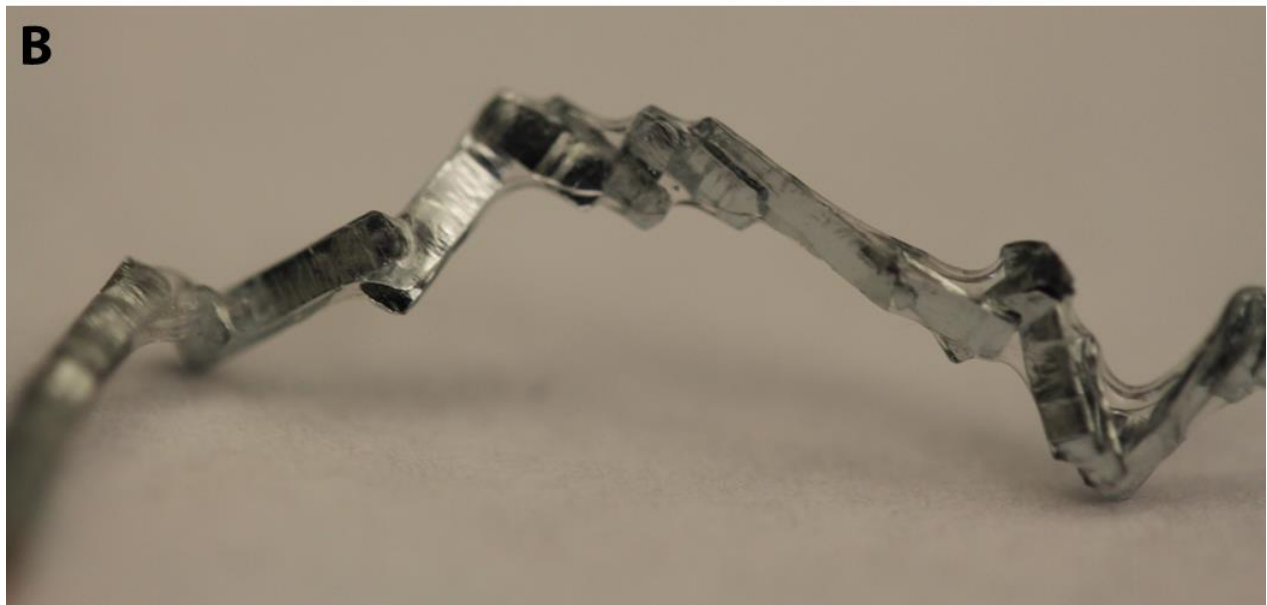


Fig. S8. Optical images of a relaxed metamaterial after straining. (A, B) Optical images of a relaxed metamaterial fiber post-straining before repairing the gallium core via heating. The outer polymer shell holds the fiber together despite the multiple fractures in the gallium core. The post-mortem analysis was completed on the gallium core segments after straining to study the deformation mechanism of the gallium in the fiber. Photo credit: Chris Cooper, North Carolina State University

Table S1. Comparison of mechanical properties with SDs, 95% confidence intervals, and sample sizes.

	Initial Modulus (MPa)	Tensile Strength (MPa)	Strain at Failure (%)	Toughness at 450% Strain (MJ/m ³)	Sample Size
Ga-only	1800 ± 800 [1060 , 2540]	12.4 ± 2 [11 , 14]	60 ± 20 [42 , 79]	5.3 ± 2 [3.5 , 7.1]	7
SEBS-only	3 ± 1 [0.5 , 5.5]	13.5 ± 0.6 [12 , 15]	860 ± 50 [736 , 984]	10.2 ± 0.8 [8.2 , 12.2]	3
Ga-SEBS	800 ± 1100 [0 , 1648]*	5.9 ± 2 [4.4 , 7.4]	450 ± 170 [319 , 581]	17.3 ± 5 [13.5 , 21.1]	9
*non-physical, negative values have been excluded from the 95% confidence interval.					

Movie S1. Elongation of a metamaterial fiber. This video shows a metamaterial fiber being strained by the extensometer to 350% strain. The video is played at 16x speed.

Movie S2. Slipping mechanism for the formation of polymer bridges. This video shows a metamaterial fiber after a break has occurred. The fiber is stretched by hand under a microscope to highlight the slipping mechanism through which the encasing polymer is transferred between the metal segments to create a polymer bridge. The video is played in real-time.

Movie S3. Demonstration of a metamaterial fiber. This video compares a hollow SEBS fiber to a metamaterial fiber when both fibers are under a constant load of approximately 5.5 N (558 grams). The video is played in real-time.